Synthesis, in vitro evaluation of antibacterial, antifungal and larvicidal activities of pyrazole/pyridine based compounds and their nanocrystalline MS (M=Cu and Cd) derivatives

Gopinath Mondal, Harekrishna Jana, Moumita Acharjya, Ananyakumari Santra, Pradip Bera, Abhimanyu Jana, Anangamohan Panja, et al.

Springer

MEDICINAL CHEMISTRY RESEARCH

CrossMark

ORIGINAL RESEARCH

Synthesis, in vitro evaluation of antibacterial, antifungal and larvicidal activities of pyrazole/pyridine based compounds and their nanocrystalline MS (M = Cu and Cd) derivatives

Gopinath Mondal[1] · Harekrishna Jana[2] · Moumita Acharjya[1] ·
Ananyakumari Santra[1] · Pradip Bera[1] · Abhimanyu Jana[1] · Anangamohan Panja[1] ·
Pulakesh Bera [1]

Abstract Methyl 3,5-dimethyl pyrazole-1-dithioate (mdpa) (**1**), benzyl 3,5-dimethyl pyrazole-1-dithioate (bdpa) (**2**), 3,5-dimethylpyrazole-1-(5methyl-1H-pyrazol-3-ylmethyl)-1H-pyrazole (**3**), copper(II)-mdpa (**4**), copper(II)-bdpa (**5**), cadmium(II)-mdpa (**6**), cadmium(II)-bdpa (**7**), Cu_2S nanoparticles (**8** and **9**) derived from **4** and **5**, respectively, CdS nanoparticles (**10** and **11**) derived from **6** and **7**, respectively, were synthesized to screen their antimicrobial activities. Prolonged reaction with $CuCl_2.2H_2O$ and **3** followed by addition of trace amount of pyridine furnished a crystalline chloro bridged complex $[Cu(\mu\text{-}Cl)_2(pyridine)_2]_n$ and its structure was solved by single X-ray crystallography. Antibacterial activities of all of the synthesized materials (**1–12**) were evaluated against Gram positive bacteria including *Staphylococcus aureus* and *Bacillus subtilis* and Gram negative bacteria including *Escherichia coli, Pseudomonas aeruginosa, Klebsiella pneumoniae* and *Proteus vulgaris*. Fungi (*Candida albicans, Aspergillus flavus*) were also used to test antifungal activities with the compounds. Present study revealed that **8** shows best antibacterial activity among the present reported compounds. An excellent antifugal activity is shown by **12** emerging to be a better antibiotic than standard fluconazole. Besides fungicidal effect, **12** has promising larvicidal effect. The structure and activity relationship has been discussed.

Keywords Antibacterial · Antifungal · Larvicidal · Pyrazole/Pyridine complexes · Nanoparticles

✉ Pulakesh Bera
pbera.pbc.chem@gmail.com

1 Post Graduate Department of Chemistry, Panskura Banamali College, Vidyasagar University, Midnapore (E), West Bengal 721152, India

2 Department of Microbiology, Panskura Banamali College, Vidyasagar University, Midnapore (E), West Bengal 721152, India

Introduction

Five member diazole viz. pyrazole, imidazole and benzimidazole are biologically very much significant. Extensive biochemical and pharmacological studies have confirmed that diazoles molecules are effective against various strains of microorganisms (Kathiravan et al. 2012; Bansal and Silakari 2012; Goker et al. 2002; Klimesova et al. 2002; Pawar et al. 2004; Boiani and Gonzalez 2005; Desai and Desai 2006; Mohammad et al. 2006; Guven et al. 2007). These are all regarded as promising class of bioactive heterocyclic compounds. Among diazoles, the pyrazole derivatives are found to be trendy scaffold used for finding of drugs in the pharmaceutical and medicinal chemistry field. The exclusive structural features of pyrazole and a vast range of biological activities of its derivatives made it privileged structure in drug discovery (Baraldi et al. 2012). The pyrazole ring systems are found in numerous antioxidant (Gouda 2015), antiimflammatory (Rao and Knaus 2008, Bekhita and Abdel-Aziem 2004), antipyretic (Malvar et al. 2014), antileishmanial (Mowbray et al. 2015), antiproliferative (Mert et al. 2014), anticonvulsant (Viveka et al. 2015), antihypertensive (Gomha et al. 2015), antineoplastic (Gupta et al. 1996), antitriclinellosis (Mavrova et al. 2007) etc. Nisha Chandna et al. prepared a series of pyrazolyl

benzyltriazoles as celecoxib analogues, which lead to the development of molecular probes for imaging of COX-2 and all the compounds were screened for in vitro and in vivo cyclooxygenase (COX) assays to determine COX-1 and COX-2 inhibitory potency (Chandna et al. 2014). Pyrazole scaffold has also emerged as a pharmacophore of choice for designing biologically active on different clinically approved targets (Camargo et al. 2015). Structural modification with further introduction of sulphur atom(s) in the pyrazole ring develops promising biological properties (Sobiesiak et al. 2014).

Not only the organic compounds but also their metal complexes sometime exhibited higher biological activities than the parent molecules. The higher activities attributed to the metal ligands interaction through several coordination and non-covalent interactions (Mitic et al. 2009; Singh et al. 2012). Several pyrazole based complexes have been reported with improved biological properties. Complexes of cobalt(II), nickel(II) and copper(II) with 2-(3,5-dimethyl-1H-pyrazole-1-yl)-4-phenyl-1,3-thiazole and 3,5-dimethyl-1H-pyrazole-1-carbothioamide were reported where authors claimed three fold higher cytotoxicity effect of the complexes against HL-60, NALM-6 leukemia cells and the WM-115 melanoma cell line than cis-platin (Sobiesiak et al. 2014).

Recent trends to develop compounds having improved properties that can be used against several microorganism borne diseases are encouraging. Besides several organic compounds and the metal complexes, the research on antibiotic development has been focused on the identification of more refined variants of existing drugs. In this context, several nanoparticles have also been used as excellent antibacterial agents (Parak et al. 2003; Tomalia 2009). Various synthetic methods were developed for size tuning, architecture manipulation and biocompatibility of nanoparticles to enhance the performance (Gao et al. 2009). Nanoparticles capped with different stabilizing agent have shown different biological activities. In continuation of our extensive work on pyrazole derivatives (Santra et al. 2016; Mondal et al. 2014; Mondal et al. 2015a, b, we report herein the synthesis, characterization and antimicrobial activities of eleven pyrazolyl compounds and one copper-pyridine derivative which is recrystallized to study the microbial activities. To our knowledge, antimicrobial study of pyrazolyl/pyridinyl compounds including their metal complexes and nanoparticles were not reported earlier to correlate the structure and activity relationship.

Material and methods

General

Reagent grade $CuCl_2 \cdot 2H_2O$, $CdCl_2 \cdot H_2O$, dimethyl sulfoxide (DMSO) and CS_2 were used without further

purification. Benzyl chloride, hydrazine hydrate (HH) and methyl iodide were purchased from Spectrochem chemical company. Analytical grade methanol, ethylene diamine (EN) and ethylene glycol (EG) were purchased from Himedia chemical company and used without further purification. Solvent ethanol (Changshu Yangyuan Chemical, China) was dried and distilled before use in the experiments.

The elemental analysis (C, H, N, and S) of the ligand and complexes were performed using FISONS EA-1108 CHN analyzer. The IR spectra (4000–500 cm^{-1}) were recorded on a Perkin Elmer Spectrum Two FT-IR Spectrophotometer with sample prepare as KBr pellets. UV–visible absorption spectra of the partitioned amount of samples were recorded on a Perkin Elmer Lambda 35 spectrophotometer in the wavelength range region 200–800 nm at room temperature. ^{1}H-NMR of the compound **3** was measured by BRUKER 400 MHz instrument and mass spectrum was obtained using a Waters HRMS XEVO-G2QTOF♯YCA 351 instrument. The single crystal X-ray diffraction (XRD) of **12** was carried out on a Bruker SMART APEX II X-ray diffractometer equipped with graphite-monochromatic Mo-Kα radiation ($\lambda = 0.71073$ Å) and 16 CCD area detector. The intensity data were collected in the π and ω scan mode, operating at 50 kV, 30 mA at 296 K (Bruker et al. 2001). The data reduction was performed using the SAINT and SADABS programs (Bruker et al. 2001). All calculations in the structural solution and refinement were performed using the Bruker SHELXTL program (Sheldrick 2001). The structure was solved by the heavy atom method and refined by full-matrix least-squares methods. All the non-hydrogen atoms were refined anisotropically; the hydrogen atoms were geometrically positioned and fixed with isotropic thermal parameters. The final electron density maps showed no significant difference.

General procedure for the synthesis of 1–12

The compound **3**, **8** and **12** are synthesized and characterized for the first time where remaining compounds re-synthesized to evaluate their biological activity. Ligand **1** (methyl 3,5-dimethyl pyrazole-1-dithioate) and **2** (benzyl 3,5-dimethyl pyrazole-1-dithioate) were resynthesized according to the earlier reported process (Mondal et al. 2014, Santra et al. 2016, Mondal et al. 2016). Scheme 1 represents the reactions steps associated in the formation of the compounds (**4–11**) from the ligands. Complex **4** and **5** were obtained by the reaction of ethanolic solution of coper (II) chloride and ligand dissolved in acetonitrile in 1:2 molar ratio (Mondal et al. 2014). Similarly complexes **6** and **7** were obtained by the reaction of cadmium(II) chloride and ligand in ethanol with mole ration 1:2 (Mondal et al. 2015a, 2015b). The details of the synthesis and characterization of ligands (**1–2**), complexes (**4–7**) and nanoparticles (**9–11**)

Scheme 1 Scheme for formation of the compounds **1–2** and **4–11** (N.B. *Dotted oval part* represents 3,5-dimethyl pyrazole (dmpz): core unit of the compounds)
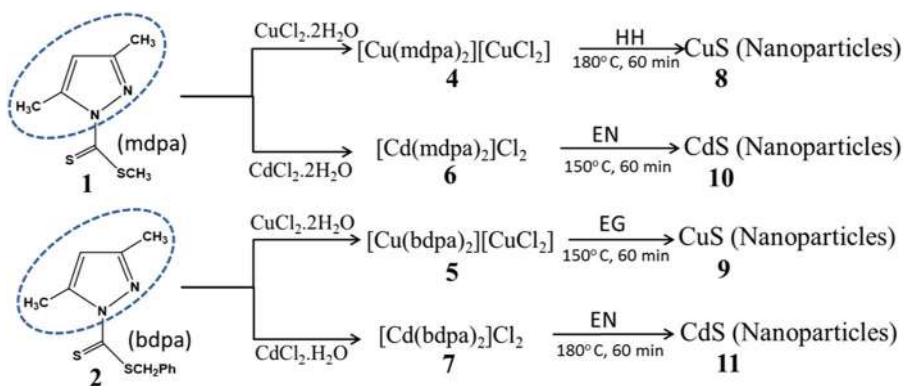
Scheme 2 Scheme for formation of the compounds **3** and **12** (N.B. *Dotted oval part* represents 3,5-dimethyl pyrazole (dmpz): core unit of the compounds)
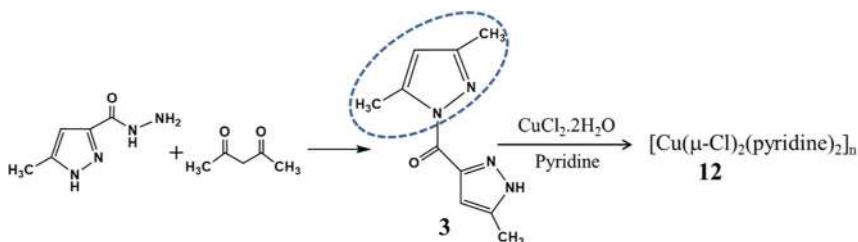
were reported earlier by us (Santra et al. 2016; Mondal et al. 2014; Mondal et al. 2015a, 2015b).

CuS nanoparticles (**8**) were synthesized in a solvothermal method taking a mixture of **4** (0.5 mmol, 0.285 g) and HH (15 mL) in a 50 mL two-necked round bottom flask equipped with a condenser and thermocouple adaptor. The flask was degassed at room temperature for 5 min and then filled with inert nitrogen gas. The resulting solution was then gradually heated to 180 °C and maintained the reaction temperature for 60 min. The black precipitate formed was collected through centrifugation and washed 4 to 5 times with ethanol. Dry powder of copper sulfide nanocrystals were collected by evaporating ethanol at 100 °C for 1 h in oven.

Compound **3** was synthesized by the condensation of equimolecular amount of 5-methyl pyrazole-3-carbohydrazide and acetyl acetone and is shown in Scheme 2. Acetyl acetone (1.04 mL 10 mmol) is added to the solution of 5-methyl pyrazole-3-carbohydrazide (Bera et al. 2009) (1.40 g, 10 mmol) dissolved in 70 mL water with constant stirring for 3 h. A white solid separates out which is filtered off and washed with distilled water. Yield 90%. Mass spectrum: Molecular ion peak (m/z) 205 (Fig. S1). Anal. calc. for $C_{10}H_{12}N_4O$,: C, 58.81, H, 5.92; N, 27.43; Found C, 58.68; H, 5.76; N, 26.91; IR/cm^{-1}: $\nu_{(C=N)}$ 1583, $\nu_{(N=N)}$ 1427. NMR (CDCl$_3$, 500 MHz): δ 12.41 (s,1 H), δ 7.20 (s, 1 H), δ 7.00 (s, 1 H), δ 2.60 (s, 3 H), δ 2.30 (s, 3 H), δ 2.20 (s, 3 H) (Fig. S2).

The ethanolic solution of **3** (10 mmol) and CuCl$_2$• 2H$_2$O (5 mmol) did not furnish any solid product on prolonged reflux (30 h). But the compound **12** is obtained from the resulting solution of **3** and CuCl$_2$•2H$_2$O on addition of pyridine. The crude product was filtered off and washed with methanol. Diffraction quality crystals are obtained from the slow evaporation of the methanolic solution of the crude product. Yield 75%. Anal. calc for $C_{10}H_{10}Cl_2CuN_2$: C, 41.04; H, 3.44; N, 9.57. Observed: C, 41.09; H, 3.41; N, 9.82. IR (cm^{-1}): $\nu_{(C=N)}$ 1640, $\nu_{(C-N)}$ 1429, $\nu_{(H2O)}$ 3480.

Determination of the logP by using the shake-flask method

The logP values of ligands and complexes were determined according to the shake-flask method [Kupcewicz et al. 2013]. Compounds under investigation were weighted out accurately and partitioned between equal volumes of water and 1-octanol (5 mL each) by shaking for 30 h at room temperature to assure full partitioning of the analyzed compounds between two water and 1-octanol phases. Then, the solution was centrifuged at 3500 rpm for 10 min to separate two layers. The concentration of the compounds in different layers was measured by the optical density values obtained from UV−vis spectroscopy.

Determination of antibacterial and antifungal activity

Antibacterial sensitivity is tested by the agar well diffusion method using Mueller–Hilton agar media. The agar diffusion method is employed for the determination of antibacterial activities of twelve pyrazolyl compounds

according to the method described by Vanden Berghe and Vlietinck 1991. The compounds under investigation are dissolved in DMSO to a final concentration 500 μg/mL. Six species of pathogenic bacteria namely *Escherichia coli*, *Klebsiella pneumoniae*, *Staphylococcus aureus*, *Proteus vulgaris*, *Pseudomonas aeruginous* and *Bacillus subtilis* are used to screen the antibacterial activity of the compounds (Nostro 2000). Pathogenic bacterial strains are incubated in sterile nutrient broth and incubated at 37 °C for 24 h. The pathogen are swabbed (inoculums size was adjusted so as to deliver a final inoculums of approximate 10^6 CFU/mL) on the surface of Mueller-Hilton agar media. The petri dishes containing 25 mL of Mueller–Hinton Agar with 100 μL inoculums of bacterial strain and media are allowed to solidify. Wells are cut into solidified agar media with the help of sterilized cup-borer. A volume of 100 μL of each sample solution is poured in the respective wells and the plates are incubated overnight at 37 °C for bacteria. DMSO and ethanol are used as control. The experiment is performed in triplicate under strict aseptic conditions and the antibacterial activity of each compound was expressed in terms of the mean diameter of zone of inhibition (cm) produced by the respective compound. The stock solution for the determination of antibacterial activity was made by dissolving the antibiotics in sterile water at a concentration 500 μg/mL. From this stock solution different concentration of working solution (ranges from 200 to 0.1 μg/mL) was prepared.

Similarly, antifungal sensitivity is tested by the agar well diffusion method using PD agar media (Nostro 2000). Two species of pathogenic fungi namely *Aspergillus flavus* and *Candida albicans* are used to screen the antifungal activity of the pyrazolyl compounds. Pathogenic fungal strain are inoculated in sterile potato dextrose broth and incubated at 25 °C for 48 to 72 h. Petri dishes containing 25 mL of Potato dextrose agar with 100 μL inoculums of fungal strain and media is allowed to solidify. The remaining work off processes is similar to that of antibacterial sensitivity test. The stock solution for the determination of antifungal activity was made by dissolving the antibiotic in sterile distilled water with concentration 500 mg/mL. Different concentrations ranging from 250 to 50 mg/mL were made from the measured amount of stock solution.

Determination of minimum inhibitory concentration (MIC) of sample

Minimum inhibitory concentration is determined using inhibitory concentration in diffusion method (Guerin-Faublee et al. 1996). The MIC values, which represent the lowest concentration of the compound that completely inhibits the growth of microorganisms, are determined by a micro-well dilution method (Wade et al. 2001). The

inoculums of each bacterium and fungus are prepared with concentration of suspension 10^6 CFU/mL. To obtain the dilution, pyrazolyl compounds are dissolved in DMSO at a higher concentration and make it dilute with measured amount of DMSO and/or ethanol to obtain concentration 200, 150, 100, 75, 50 μg/mL, 20, 15, 10, 5, 3 mg/mL. A volume of 100 μL of compound of different concentration is poured in the respective wells and the plates are incubated 96 h at 28 °C for fungi and 24 h at 37 °C for bacteria. The experiment is repeated three times under strict aseptic conditions.

Determination of larvicidal activity of sample

The larvicidal bioassay follows the World Health Organization standard protocols (WHO, 1981) along with a set of control containing distilled water without any test solution. Required concentrations of different sample solutions are prepared through the mixing of stock solution with variable amount of DMSO. Each of the earlier prepared compounds was transferred into the test tubes. The larvae of *Culex quinquefasciatus* (*Cx. quinquefasciatus*) are separately introduced into different test tubes containing appropriate concentrations. Mortality rates are recorded after 24, 48 and 72 h of post-exposures. Dead larvae were identified when they failed to move after probing with a needle in the siphon or cervical region. All the data was analyzed statistically using SPSS-10.0. Each sample was analyzed and data were represented as mean ± SD.

Results and discussion

As ligand, pyrazole derivatives have attracted considerable interest mainly because of their variety of coordination modes with metals and have effective interactions with biological molecules like proteins, nucleic acids etc. (Castro et al. 2011; Kaur et al. 2014; Blaszczak-Swiqtkiewicz and Mikiciuk-Olasik 2015; Porcari et al. 1998). Sobiesiak et al. reported that the presence of carbothio amide in the structure improved the activity of the compound significantly (Sobiesiak et al. 2014). Mono dentate 3,5 dimethyl pyrazole (dmpz) can be converted to a bidentate ligand (**1** and **2**) by the addition of dithioate group in the N(1) position of dmpz (Scheme 1). The ligands (1 and 2) act as NS chelator when coordinate with metal ion. The detailed synthetic outlines of all compounds are presented in Schemes 1 and 2. The substitution of bulky keto (5-methyl pyrazole) group in N1 position of dmpz introduces two more coordination sites in **3** (Scheme 2) and additionally imparts steric congestion in the structure. Further reaction of ligands with metal salt like copper chloride and cadmium chloride produces metal complexes of different structural compositions. It is
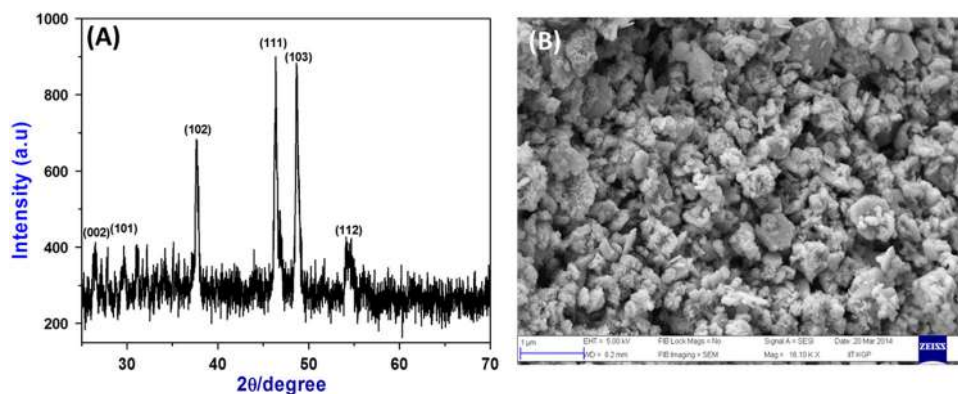
Fig. 1 a XRD and **b** SEM images of the sample **8**

observed that the metal complexes have lesser antimicrobial activities than corresponding uncoordinated ligand. The electron density of sulfur atom in the ligand molecule is reduced on coordination with the metal and hence the interacting tendency of sulfur with the protein molecules reduces significantly.

Now-a-days, the nanoparticle synthesis using single-source precursor (SP) has been popularized because the SP-method is simple and ecofriendly, where solvothermal decomposition of SP furnishes the desired nanoparticles. Moreover, the above decomposition process can be done at lower temperature than the available methods of nano-particles synthesis (Malik et al. 2010; Nyamen et al. 2013). We prepared copper sulfide and cadmium sulfide nano-particles using SP **1** and **2** at different reaction conditions. The details of synthesis and characterization of nano-particles were reported earlier by us except **8**. Figure 1a shows the powder XRD pattern of sample **8** which matches well with the standard sample of copper sulfide (JCPDS card 26-1116). The XRD pattern reveals that the sample **8** is microcrystalline chalcosite copper sulfide. Figure 1b shows the SEM picture of **8**. The 3D flower like architecture with porosity is found in the structure of **8**. The porous 3D architecture of **8** may have active sites to exhibit higher antibacterial and larvicidal activity. The same explanation may holds good for sample **9**, **10** and **11** (Fig. S3).

Unlike **1** and **2**, ligand **3** did not furnish any solid with $CuCl_2 \cdot H_2O$. However, the addition of pyridine to the resulting refluxed solution of **3** and $CuCl_2 \cdot H_2O$ produced a Cl-bridged polymeric complex, $[Cu(\mu\text{-}Cl)_2(Pyridine)_2]_n$ (**12**). The structure was solved by means of single X-ray crystallography. The concomitant formation of pyridyl bridged complex might be due to the favorable steric profile of the complex. The possible mode of bindings of ligand **3** to the metal centre may occur either through ring nitrogen of one pyrazole or by through NN atoms of both the pyr-azoles. The later rendered high steric congestion in the copper centre (atomic radius 75 pm) thus disfavor the
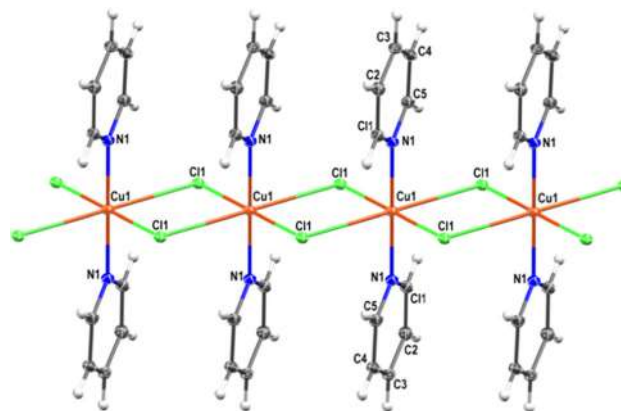
Fig. 2 Double chloride-bridged copper(I) chain structure of **12**

complex formation with **3**. Higher concentration of the bulkier ligand (**3**) presence in the reaction solution may stabilize the Cu_2Cl_2 bridged structure only allowing rela-tively small coordinating molecules e.g., pyridine to satisfy the remaining secondary valences. Pyridine is a smaller ligand and good electron donor than **3**. Thus pyridine can effectively coordinate and stabilize the bridged complex (**12**) where bulky pyrazole derivative (**3**) fails to form such bridged Cu(II) complex. Therefore the substitution in N1 position of 3,5-dimethyl pyrazole (dmpz) with bulky group as in **3** is inappropriate to form stable complex. The struc-ture of **12** is solved by single X-ray crystallography. Lit-erature survey showed that the reaction of $CuCl_2$ and pyridine formed complex species that existed in solution only (Roubaty et al. 1977). However, J. D. Dumitz reported crystal structure of copper dipyridine dichloride with sym-metric copper centre (Dumitz 1957).

Description of crystal structure

The structure of $[Cu(\mu\text{-}Cl)_2(Pyridine)_2]_n$ (**12**) have been determined by single crystal XRD method. The perspective view of molecular structures of **12** is depicted in Fig. 2, and

Table 1 Crystal data and refinement parameters of [Cu(μ-Cl)₂(pyridine)₂]ₙ (**12**)

Empirical formula	$C_{10} H_{10} Cl_2 Cu N_2$
Formula weight	292.65
Temperature	100 K
Dx (g cm⁻³)	1.777
Crystal system	Monoclinic
Volume	546.86(3)
Space group	P 21/n
a (Å)	3.7882(1)
b (Å)	8.5078(3)
c (Å)	16.9770(6)
α (°)	90
β (°)	91.900(2)
γ (°)	90
Z	2
Mu (mm⁻¹)	2.449
F000	294.0
F000'	295.28
h,k,l max	5,11,22
Nref	1354
Theta (max)	28.340
R (reflections)	0.0179(1260)
wR2 (reflections)	0.0465(1351)

Table 2 Selected bond length and bond angles of [Cu(μ-Cl)₂(pyridine)₂]ₙ (**12**)

Bond Angles (°)				Bond Lengths (Å)		
Atom1	Atom2	Atom3	Angle (°)	Atom1	Atom2	Length(Å)
Cu1	Cl1	Cu1	91.17(1)	Cl1	Cu1	2.3065(3)
Cl1	Cu1	N1	90.42(3)	Cl1	Cu1	2.9585(3)
Cl1	Cu1	Cl1	180.00(1)	Cu1	N1	2.009(1)
Cl1	Cu1	N1	89.58(3)	Cu1	Cl1	2.3065(3)
Cl1	Cu1	Cl1	91.17(1)	Cu1	N1	2.009(1)
Cl1	Cu1	Cl1	88.83(1)	Cu1	Cl1	2.9585(3)
N1	Cu1	Cl1	89.58(3)	Cu1	Cl1	2.9585(3)
N1	Cu1	N1	180.00(5)	N1	C1	1.343(2)
N1	Cu1	Cl1	89.61(3)	N1	C5	1.345(2)
N1	Cu1	Cl1	90.39(3)	C2	C1	1.384(2)
Cl1	Cu1	N1	90.42(3)	C2	C3	1.390(2)
Cl1	Cu1	Cl1	88.83(1)	C2	H2	0.95(2)
Cl1	Cu1	Cl1	91.17(1)	C1	H1	0.94(2)
N1	Cu1	Cl1	90.39(3)	C5	C4	1.384(2)
N1	Cu1	Cl1	89.61(3)	C5	H5	0.94(2)
Cl1	Cu1	Cl1	180.00(1)	C4	C3	1.386(2)
Cu1	N1	C1	121.58(9)	C4	H4	0.93(2)
Cu1	N1	C5	120.03(9)	C3	H3	0.94(2)

the crystal parameter and selected bond lengths and angles are given in Table 1 and Table 2. The crystal structure of **12** is constructed 1D polymers consisting of doubly bridged metal centers with Cl atoms. In the chain, Cu…Cu separation is 3.788 Å. The geometry of the complex is six coordinated with somewhat distorted octahedral geometry as reflected from the significant deviation of the *cisoid* and *transoid* angles from the ideal values. The coordination environment of Cu is completed by two pyridine ligands, displayed in *trans* positions. Being the weaker field ligand than the pyridine, chloride occupies the axially elongated trans positions of Cu(II) center. In the chain, Cu₂Cl₂ bridging unit lies in the same plane rendering the system to be perfectly planer. In absence of conventional proton on N in pyridine, the intra chain hydrogen bonding interactions between bridging chlorides and ligand are absent. Therefore, the arrangement of the chain structure is not energetically favorable like other similar pyrazolyl based structure (Santra et al. 2016, Albada et al. 2008) with hydrogen bonding interactions. Therefore, the chain structure is stabilized by the intermolecular hydrogen bonding and π–π interactions. Due to the lack of conventional hydrogen bonding ability of pyridine group it cannot stabilize the helical chain structure rather prefer to yield straight chain structure in order to minimize steric congestion. Thus it can

be safely concluded that the linear chain structure of **12** has more penetration to the folded protein in the biological systems. This property may explain the good antimicrobial activity of **12** (Table 3).

Antimicrobial activity

The efficiency of antibacterial and antifungal effects of any compound (natural or synthetic) depends on the penetration power of the compound to the organisms. The mechanism of action of antifungal and antibacterial resistance to them is limited by several factors (Tavares et al. 2013). The structures of fungi and bacteria differ in very significant ways such as the diploid nature of most fungi and the longer generation time of fungi compared to bacteria, and the available antibacterial/antifungal agents target structures and functions or both which are relevant to the inhibitory activity of the organisms. For example, many antibacterial agents inhibit the formation of peptidoglycan, the essential component of the bacterial cell wall. For other types of bacterial resistance where the comparisons are limited to the antifungal analogue with respect to protein synthesis inhibitors (amino glycosides, macrolides and tetracyclines), topoisomerase inhibitors (fluoroquinolones) and metabolic pathway inhibitors (trimethoprim-sulfamethoxazole). In contrast, most antifungal compounds target the formation and function of ergosterol (an important component of the

fungal cell membrane). Understanding the mechanism(s) of action of different antimicrobial agents is an important prerequisite to understand mechanisms of resistance. In fact, in many cases an elucidation of resistance mechanisms has allowed or enhanced understanding of specific mechanisms of action (Raman et al. 2006). The results in the present in vitro antimicrobial activities of the ligands **1–3**, the metal complexes **4–7**, **12** and nanoparticles **8–11** are presented in Table 3, and the MIC values of **1**, **3**, **8** and **12** are given in Table 4. The results of sensitivity test of some standard

Table 3 Antimicrobial activity of specific concentration (500 μg/mL) of different synthesized compounds and antibiotics with control by agar well diffusion method

Sample	Zone of inhibition (in cm) against							
	Bacteria						Fungi	
	E. coli Mean ± SD	B. subtilis Mean ± SD	K. pneumoniae Mean ± SD	P. vulgaris Mean ± SD	S. aureus Mean ± SD	P. aeruginosa Mean ± SD	A. flavus mean ± SD	C. albicans mean ± SD
1	1.9 ± 0.03	1.2 ± 0.05	1.2 ± 0.05	1.5 ± 0.05	1.3 ± 0.05	1.4 ± 0.01	1.5 ± 0.05	2.0 ± 0.01
2	1.3 ± 0.01	1.2 ± 0.01	1.1 ± 0.05	1.2 ± 0.05	1.3 ± 0.01	1.1 ± 0.06	1.4 ± 0.05	1.4 ± 0.05
3	2.0 ± 0.05	2.0 ± 0.05	1.6 ± 0.01	1.1 ± 0.05	1.3 ± 0.05	1.4 ± 0.05	1.4 ± 0.01	1.4 ± 0.05
4	1.4 ± 0.03	1.2 ± 0.05	1.2 ± 0.01	1.2 ± 0.01	1.2 ± 0.01	1.2 ± 0.06	1.2 ± 0.01	1.4 ± 0.01
5	1.5 ± 0.01	1.2 ± 0.11	1.2 ± 0.05	1.1 ± 0.05	1.2 ± 0.05	1.2 ± 0.06	1.2 ± 0.05	1.1 ± 0.05
6	1.3 ± 0.01	1.2 ± 0.01	1.2 ± 0.05	1.2 ± 0.05	1.3 ± 0.01	1.2 ± 0.06	1.2 ± 0.03	1.5 ± 0.05
7	1.3 ± 0.05	1.2 ± 0.05	1.2 ± 0.01	1.2 ± 0.01	1.6 ± 0.01	1.1 ± 0.01	1.3 ± 0.01	1.6 ± 0.05
8	3.0 ± 0.05	1.2 ± 0.05	3.0 ± 0.01	2.5 ± 0.05	1.3 ± 0.05	1.2 ± 0.06	1.9 ± 0.03	2.1 ± 0.01
9	1.3 ± 0.01	1.3 ± 0.01	1.2 ± 0.05	1.2 ± 0.01	1.5 ± 0.01	1.2 ± 0.06	1.6 ± 0.01	2.0 ± 0.05
10	2.6 ± 0.05	1.2 ± 0.05	1.3 ± 0.01	1.3 ± 0.01	1.3 ± 0.01	1.2 ± 0.01	1.4 ± 0.05	1.5 ± 0.01
11	1.3 ± 0.01	1.2 ± 0.05	1.5 ± 0.05	1.2 ± 0.01	1.3 ± 0.01	1.0 ± 0.06	1.3 ± 0.05	1.4 ± 0.01
12	1.9 ± 0.04	2.2 ± 0.05	1.9 ± 0.05	1.9 ± 0.05	1.7 ± 0.05	1.8 ± 0.01	2.6 ± 0.05	3.0 ± 0.05
Flucanazole							1.9 ± 0.17	1.1 ± 0.057
Griseofulvin							2.3 ± 0.2	2.1 ± 0.057
Control								
DMSO	1.3 ± 0.05	1.2 ± 0.05	0.9 ± 0.05	1.1 ± 0.05	1.3 ± 0.05	1.2 ± 0.06	1.3 ± 0.05	1.4 ± 0.05
EtOH	1.2 ± 0.05	1.2 ± 0.05	0.9 ± 0.05	1.2 ± 0.05	1.2 ± 0.05	1.2 ± 0.06	1.2 ± 0.05	1.0 ± 0.05

N.B: **4** and **5** are soluble in ethanol and all other samples are soluble in dimethyl sulfoxide. SD- Standard deviation

Table 4 MIC (minimum inhibitory concentration) value of different compounds and antibiotics against different bacteria and fungi

Sample No	MIC value of sample							
	Bacteria (μg/mL)						Fungi (mg/mL)	
	E. coli	B. subtillis	K. pneumoniae	P. vulgaris	S. aureus	P. aeruginosa	A. flavus	C. albicans
1	100	Fungi (mg/mL)	–	50	–	–	5	3
3	75	75	100	–	–	100	–	–
8	150	–	75	50	–	–	10	20
12	75	100	100	75	100	100	20	15
Azithromycin	–	1	0.25	0.5	25	1		
Amoxicillin	2	50	10	10	25	2		
Ampicillin	20	40	10	5	–	8		
Chloramphenicol	–	5	10	–	25	5		
Ciprofloxacin	8	5	2	0.5	25	0.1		
Cefuroxime	–	1.5	–	3	–	75		
Doxycyclin	–	3	–	5	3	2		
Ofloxacin	8	3	–	3	5	8		

pathogenic bacteria and fungi against basic ligand dmpz (500 µg/mL) and DMSO (control) are given in the Table 5. Camera views of the experiments on agar are provided in the supplementary data (Figs. S5–S12). The antimicrobial activities of the ligands (**1–2**) are greater than the parent ligand 3,5-dimethyl pyrazole (dmpz). This result indicates that the dithioate group (–SR) of **1** and **2** hydrolyzes into –SH group in the biological system. The –SH group can increase the lipophilic property of the compound (Ansari and Lal 2009a, 2009b). This lipophilicity of the molecules plays an essential role in showing antimicrobial effect. This property is observed as an important parameter related to membrane permeation in biological system. Many of the process of drug disposition depend on the capability to cross membranes and hence there is a high correlation with lipophilic character of the compound [Kupcewicz et al. 2013]. The log$P$ values of some representative compounds are given in Table 6. The general trend of the logP values reveals that lipophilicity of ligand (**1** and **2**) is greater than corresponding metal complexes (**4–7**). It is also found that the sensitivities of the ligands (**1–3**) are greater than the corresponding copper and cadmium complexes (**4–7**). This fact can be explained by the reduction of the polarity of the pyrazolyl ligands on bonding with metal centers which also

is reflected by the log$P$ value (Table 6). There are many examples in literature where activities of many ligands decrease on coordination (Roy et al. 2007; Roy et al. 2007). However, the zone of inhibition of the investigated strains of gram negative bacteria caused by the complexes are compared in the order as follows: Cu(I)-complex (**4** and **5**) > Cd(II)-complex (**6** and **7**). The copper complexes (**4** and **5**) contains easily oxidizable Cu(I) centers which might have better ability to inhibit the synthesis of bacterial cell wall than Cd(II) complexes. The opposite trend in the antifungal activity was observed. The reason simply may be the poisonous effect of cadmium ion to the synthesis of ergosterol in the fungal cell membrane. It is to be noted that copper, an essential trace element has no toxic effect but the cadmium has toxic effect beyond certain limit. In our experiment, trace amount of cadmium salt is used for the preparation of stable cadmium complexes which are not likely to be toxic enough. On the other hand, the tested pyrazolyl compounds are expected to be nontoxic to the living system as numerous pyrazole derivatives were used as safe drugs against human diseases (Bekhita and Abdel-Aziem 2004, Roy et al. 2007).

The best antifungal activity was shown by **12** among the studied materials (Table 3). The best activity of **12** was

Table 5 Sensitivity test of some Pathogenic bacteria and fungi against ligand 3,5-dimethyl pyrazole (dmpz) (500 µg/mL) and DMSO (control)

Name of microorganism	dmpz (cm)	DMSO
E. coli	1.3 ± 0.05	1.3 ± 0.05
B. subtilis	1.2 ± 0.05	1.2 ± 0.05
K. pneumoniae	0.9 ± 0.05	0.9 ± 0.05
P. vulgaris	1.4 ± 0.05	1.1 ± 0.05
S. aureus	1.3 ± 0.05	1.3 ± 0.05
P. aeruginosa	1.2 ± 0.05	1.2 ± 0.05
A. flavus	1.3 ± 0.05	1.3 ± 0.05
C. albicans	1.4 ± 0.05	1.4 ± 0.05

Table 7 MIC value of different antibiotics ranges from (250–50 mg/mL) against different pathogenic fungi

Name of fungi	Concentration	Antimicrobial zone (cm)	
		Griseofulvin	Flucanazole
Candida albicans	250 mg/mL	2.1	1.1
	150 mg/mL	1.5	–
	100 mg/mL	1.3	–
	50 mg/mL	–	–
Aspergillus flavus	250 mg/mL	2.3	1.9
	150 mg/mL	1.9	1.2
	100 mg/mL	–	–
	50 mg/mL	–	–

Table 6 log$P$ values of some representative compounds

Sample	1-Octanol		Water		log$P$
	Concentration (g/L)	Absorbance	Concentration (g/L)	Absorbance	
dmpz	2.58	0.504	4.8	0.9664	−0.285
1	5.14	2.293	0.78	0.351	0.817
2	5.53	2.851	0.58	0.315	0.979
3	1.21	0.828	0.54	0.219	0.347
4	5.50	1.961	0.92	0.328	0.776
5	1.56	0.817	0.46	0.269	0.531
6	1.45	1.787	0.72	0.893	0.301
7	1.61	1.526	0.52	0.654	0.491
12	0.87	0.572	0.19	0.120	0.661

Table 8 Shape and size of the nanoparticles **8–11**

Sample no.	Nanoparticles (capping agent)	Phase	Shape	Size (nm)
8	Copper sulfide (HH)	Chalcosite	Hexagonal	60
9	Copper sulfide (EN)	$Cu_{1.9}S$	Spherical	17
10	Cadmium sulfide (EG)	CdS	Spherical	10
11	Cadmium sulfide (EN)	CdS	Rod	80[a]/10[b]

Solvents act as capping agent

[a] Average length, [b] Average diameter

observed against the yeast *A. flavous* and *C. albicans* with the zones of inhibition 26 and 30 mm, respectively, which are higher than the zone inhibition 19 and 11 mm, respectively, of the standard drug fluconazole (Table 3). Chloro bridged complex (**12**) shows excellent antifungal activity against *A. flavus* and *C. albicans* with MIC value 20 and 15 mg/mL, respectively emerging to be a better antibiotic than standard fluconazole which possesses the MIC value 150 and 250 mg/mL against *A. flavus* and *C. albicans*, respectively (Table 7). The straight chain structure of the complex **12** with loosely bound pyridine molecules in the axial position might have better penetration to the cell wall of microorganism. The complex is expected to be labile with respect to de-pyridination giving a straight chain structure of bridged Cu_2Cl_2 moiety. The Cu centres of Cu_2Cl_2 straight chain may now very much effective to reduce the function of ergosterol where the free pyridine may act as effective medium for copper and DNA interaction. The relatively high logP value of **12** also attested the superiority as an antifungal agent.

The nanoparticles (**4–7**) derived from the complexes are also screened to check their antimicrobial activities. The details of shape, size and phase of the reported nanoparticles along with **8** are listed in Table 8 for ready reference. The XRD and SEM images of **9**, **10** and **11** are provided in Fig. S3. All these nanoparticles show better activity than the primary ligand dmpz. The Cu_2S nanoparticles (**8**) synthesized from **4** using HH solvent emerges as the best antibacterial agents among the tested nanoparticles. Nanoparticle **8** has maximum antibacterial activity against *E. coli* (30 mm) and *K. pneumonia* (30 mm) (Table 3) at an MIC of 150 and 75 μg/mL (Table 4), respectively which has greater MIC values than the standard antibiotic ciprofloxacin with values 8 μg/mL against *E. coli* and 2 μg/mL against *K. pneumonia* (Table 4). The reason may be due to the small size (60 nm) (Fig. S4), platelet morphology of the particle and the shorter wettibility of HH than bivalent solvent like EN and EG. The shorter wettibility also causes anisotropic growth of NCs. The small sizes of the particles enhance the permeability through the cell membrane of the microorganisms where the short amine in the surface enhances the solubility of the particles in the cell

Table 9 Determination of antilarval activity of samples

Sample Name	Concentration (μg /mL)	Rate of viability			
		0 h % Viable	24 h % viable	48 h % viable	72 h % viable
1	500	100	90	10	0
2	500	100	20	20	0
3	500	100	100	0	0
8	500	100	100	0	0
12	500	100	80	0	0
Control	–	100	100	100	100

membrane. Additionally, the platelet morphology can have an easy access in the folded protein structure of the microorganism to resist the normal functions of protein. The result shows that the short ammine capped nanoparticles have better antibacterial activity than ethylene glycol capped sample, e.g., **9**. Now it can be argued that the mechanism of action of organic compounds and their metal complexes are different than that of nanoparticles. The penetration of cells by the former largely depends upon the lipophilicity where the small size of nanoparticles which ensure the high surface energy, is the quality for cell penetration.

From the result of the preliminary screening of the tested compounds, we choose compound **1**, **2**, **3**, **8**, and **12** to examine larvicidal activity against larvae of *Cx. quinquefasciatus*. The results are given in the Table 9. It was interesting to note that the compound **12** shows best larvicidal activity where the retention of larvae is 80 % and 0 % after 24 and 48 h, respectively. Besides **12**, Compound **8** has also comparable larvicidal effect where 0% retention of larvae is also observed after 48 h.

Conclusion

Pyrazolyl and pyridinyl derivatives including ligands, metal complexes and nanoparticles are evaluated with respect to antibacterial, antifungal and larvicidal activities. All the

synthesized compounds exhibit antimicrobial activities towards selected bacteria and fungi. Substitution in N(1) position of pyrazole with carbodithioate group increases the lipophilicity which proportionately enhances the antibacterial activities. The reduced antibacterial activities of corresponding metal complexes is due to the reduction of electron density on 'S' and 'N' atoms upon complexation. The ammine capped metal sulfide nanoparticles (**8**) shows maximum antibacterial activity. Linear chain compound (**12**) with Cu_2Cl_2 distorted ring unit exhibits excellent antifungal and larvicidal effect emerging to be a better antibiotic than standard fluconazole. The pyrazole based ligands with N(1) substitution with sulfur as dithioate and bridged Cu_2Cl_2 moiety may be used as pharmacophore in drug development. Further the complexes with bridged Cu_2Cl_2 moiety can be used to remove the epidemic *culex* mosquito from environment.

Compliance with ethical standards

Conflict of interest The authors declare that they have no competing interests.

References

Albada GA, Horst MG, Mutikainen I, Turpeinen U, Reedijk J (2008) New 3,5-dimethylpyrazole copper(II) compounds with a variety of hydrogen bonds, synthesized by using a dehydrating agent: Synthesis, characterization, structures and intermolecular interactions. Inorg Chim Acta 361:3380–3387

Ansari KF, Lal C (2009a) Synthesis, physicochemical properties and antimicrobial activity of some new benzimidazole derivatives. Eur J Med Chem 44:4028–4033

Ansari KF, Lal C (2009b) Synthesis, physicochemical properties and antimicrobial activity of some new benzimidazole derivatives. Eur J Med Chem 44:2294–2299

Bansal Y, Silakari O (2012) The therapeutic journey of benzimidazoles: a review. Bioorg Med Chem 20:6208–6236

Baraldi PG, Saponaro G, Tabrizi MA, Baraldi S, Romagnoli R, Moorman AR, Varani K, Borea PA, Preti D (2012) Pyrrolo- and pyrazolo-[3,4-e][1,2,4]triazolo[1,5-c]pyrimidines as adenosine receptor antagonists. Bioorg Med Chem 20:1046–1059

Bekhita AA, Abdel-Aziem T (2004) Design, synthesis and biological evaluation of some pyrazole derivatives as anti-inflammatory-antimicrobial agents. Bioorg Med Chem 12:1935–1945

Bera P, Baek IC, Seok SI, Saha N (2009) Synthesis and spectroscopic characterization of new iron(III) complexes of S-Alkyl/Aryl dithiocarbazates of 5-methyl-3-formylpyrazole and 5-methyl-3-formylpyrazolyl-thiosemicarbazones. Russ J Coord Chem 35:526–533

Blaszczak-Swiqtkiewicz K, Mikiciuk-Olasik E (2015) Some characteristics of activity of potential chemotherapeutics–benzimidazole derivatives. Adv Med Sci 60:125–132

Boiani M, Gonzalez M (2005) Imidazole and benzimidazole derivatives as chemotherapeutic agents. Mini Rev Med Chem 5:409–424

Bruker, SAINT (Version 6.28a) and SADABS (Version 2.03) (2001) Data reduction and absorption correction program. Bruker AXS Inc, Madison, Wisconsin

Bruker, SMART (Version 5.625) (2001) Data collection program. Bruker AXS Inc., Madison, Wisconsin

Camargo TP, Maia FF, Chaves C, de Souza B, Bortoluzzi AJ, Castilho N, Bortolotto T, Terenzi H, Castellano EE, Haase W, Tomkowicz Z, Peralta RA, Neves A (2015) Synthesis, characterization, hydrolase and catecholase activity of a dinuclear iron(III) complex: catalytic promiscuity. J Inorg Biochem 146:77–88

Castro AR, Rivera IL, Rojas LC, Vazquez GN, Rodrı´guez AN (2011) Synthesis and preliminary evaluation of selected 2-aryl-5 (6)-nitro-1H-benzimidazole derivatives as potential anticancer agents. Arch Pharm Res 34:181–189

Chandna N, Kapoor JK, Grover J, Bairwa K, Goyalc V, Jachak SM (2014) Pyrazolyl benzyltriazoles as cyclooxygenase inhibitors: synthesis and biological evaluation as dual anti-inflammatory and antimicrobial agents. New J Chem 38:3662–3672

Desai KG, Desai KR (2006) Green route for the heterocyclization of 2-mercaptobenzimidazole into β-lactam segment derivatives containing −CONH− bridge with benzimidazole: screening in vitro antimicrobial activity with various microorganisms. Bioorg Med Chem 14:8271–8279

Dumitz JD (1957) The crystal structures of copper dipyridine dichloride and the violet form of cobalt dipyridine dichloride. Acta Cryst 10:307–313

Gao J, Gu H, Xu B (2009) Multifunctional magnetic nanoparticles: design, synthesis and Biological Applications. Acc Chem Res 42 (8):1097–1107

Gao J, Xu B (2009) Application of Nano materials inside cell. Nano Today 4:37–51

Goker H, Kus C, Boykin DW, Yildiz S, Altanlar N (2002) Synthesis of some new 2-substituted-phenyl-1H-benzimidazole-5-carbonitriles and their potent activity against Candida species. Bioorg Med Chem 10:2589–2596

Gomha S, Khalil K, Abdel-aziz H, Abdalla MM (2015) Synthesis and antihypertensive α-blocking activity evaluation of thiazole derivatives bearing pyrazole moiety. Heterocycles 91(9):1763–1773

Gouda MA (2015) Synthesis and antioxidant evaluation of some novel thiophene, pyrazole, chromene, pyrazolotriazine derivatives bearing sulfonamide moiety. J Heterocycl Chem. doi:10.1002/jhet.2576

Guerin-Faublee V, Muller MLD, Vigneulle M, Flandrois JP (1996) Application of a modified disc diffusion technique to antimicrobial susceptibility testing of Vibrio anguillarum, Aeromonassalmonicida clinical isolates. Vet Microbiol 51:137–149

Gupta R, Pathak D, Jindal DP (1996) Synthesis and biological activity of azasteroidal [3,2-c]- and [17,16-c]pyrazoles. Eur J Med Chem 31:241–247

Guven OO, Erdogan T, Goker H, Yildiz S (2007) Synthesis and antimicrobial activity of some novel phenyl and benzimidazole substituted benzyl ethers. Bioorg Med Chem Lett 17:2233–2236

Kathiravan MK, Salake AB, Chothe AS, Dudhe PB, Watode RP, Mukta MS, Gadhwe S (2012) The biology and chemistry of antifungal agents: a review. Bioorg Med Chem 20:5678–5698

Kaur G, Kaur M, Silakari O (2014) Benzimidazoles: an ideal privileged drug scaffold for the design of multitargeted anti-inflammatory ligands. Mini Rev Med Chem 14:747–767

Klimesova V, Koci J, Pour M, Stachel J, Waisser K, Kaustova J (2002) Synthesis and preliminary evaluation of benzimidazole derivatives as antimicrobial agents. Eur J Med Chem 37:409–418

Kupcewicz B, Ciolkowski M, Karwowski BT, Rozalski M, Krajewska U, Lorenz IP, Mayer P, Budzisz E (2013) Copper(II) complexes with pyrazole derivatives–synthesis, crystal structure, DFT calculations and cytotoxic activity. J Mol Struct 1052:32–37

Malik MA, Afzaal M, O'Brien P (2010) Precursor chemistry for main group elements in semiconducting materials. Chem Rev 110 (7):4417–4446

Malvar DC, Ferreira RT, de Castro RA, de Castro LL, Freitas AC, Costa EA, Florentino IF, Mafra JC, de Souza GE, Vanderlinde FA (2014) Antinociceptive, anti-inflammatory and antipyretic effects of 1,5-diphenyl-1H-Pyrazole-3-carbohydrazide, a new heterocyclic pyrazole derivative. Life Sci 95(2):81–88

Mavrova AT, Denkova P, Tsenov YA, Anichina KK, Vutchev DI (2007) Synthesis and antitrichinellosis activity of some bis(benzimidazol-2-yl)amines. Bioorg Med Chem 15:6291–6297

Mert S, Yağlıoğlu AŞ, Demirtas I, Kasımoğullar R (2014) Synthesis and antiproliferative activities of some pyrazole-sulfonamide derivatives. Med Chem Res 23:1278–1289

Mitic D, Milenkovic M, Milosavljevic S, GoCevac D, Miodragovic Z, AnCelkovic K, Miodragovic D (2009) Synthesis, characterization and antimicrobial activity of Co(II), Zn(II) and Cd(II)complexes with N-benzyloxycarbonyl-S-phenylalanine. Eur J Med Chem 44:1537–1544

Mohammad BG, Hussien MA, Abdel-Alim AA, Hashem M (2006) Synthesis and antimicrobial activity of some new 1-alkyl-2-alkylthio-1,2,4-triazolobenzimidazole derivatives. Arch Pharm Res 29:26–33

Mondal G, Bera P, Santra A, Jana S, Mondal T, Seok SI, Mondal A, Bera P (2014) Precursor-driven selective synthesis of hexagonalchalcocite (Cu$_2$S) nanocrystals: structural, optical, electrical and photocatalytic properties. New J Chem 38:4774–4782

Mondal G, Acharjya M, Santra A, Bera P, Jana S, Pramanik NC, Mondal A, Bera P (2015a) A new pyrazolyldithioate function in theprecursor for the shape controlled growth of CdS nanocrystals: optical and photocatalytic activities. New J Chem 39:9487–9496

Mondal G, Jana S, Santra A, Acharjya M, Bera P, Chattopadhyay D, Mondal A, Bera P (2015b) Single-source mediated facile electrosynthesis of p-Cu$_2$S thin films on TCO (SnO$_2$:F) with enhanced photocatalytic activities. RSC Adv 5:52235–52242

Mondal G, Santra A, Bera P, Acharjya M, Jana S, Chattopadhyay D, Mondal A, Seok SI, Bera P (2016) A pyrazolyl-based thiolato single-source precursor for the selective synthesis of isotropic copper-deficient copper(I) sulfide nanocrystals: synthesis, optical and photocatalytic activity. J Nanopart Res 18:311. doi:10.1007/s11051-016-3538-3

Mowbray CE, Braillard S, Speed W, Glossop PA, Whitlock GA, Gibson KR, Mills JE, Brown AD, Gardner JM, Cao Y, Hua W, Morgans GL, Feijens PB, Matheeussen A, Maes LJ (2015) Novel amino-pyrazole ureas with potent in vitro and in vivo antileishmanial activity. J Med Chem 58(24):9615–9624

Nostro A (2000) Extraction methods and bioautography forevaluation of medicinal plant antimicrobial activity. Lett Appl Microbiol 30 (1):379–384

Nyamen LD, Revaprasadu N, Pullabhotla RVSR, Nejo AA, Ndifon PT, Malik MA, O'Brien P (2013) Synthesis of multi-podal CdS nanostructures using heterocyclic dithiocarbamato complexes as precursors. Polyhedron 56:62–70

Parak WJ, Gerion D, Pellegrino T, Zanchet D, Micheel C, Williams SC et al. (2003) Biological applications of colloidal nanocrystals. Nanotechnology 14:15–27

Pawar NS, Dalal DS, Shimpi SR, Mahulikar PP (2004) Studies of antimicrobial activity of N-alkyl and N-acyl 2-(4-thiazolyl)-1H-benzimidazoles. Eur J Pharm Sci 21:115–118

Porcari AR, Devivar RV, Kucera LS, Drach JC, Townsend LB (1998) Design, synthesis, and antiviral evaluations of 1-(substituted benzyl)-2-substituted-5,6-dichlorobenzimidazoles as nonnucleoside analogues of 2,5,6-trichloro-1-(b-D-ribofuranosyl)benzimidazole. J Med Chem 41:1252–1262

Raman N, Joseph J, Velan AS, Pothiraj C (2006) Antifungal activities of biorelevant complexes of copper(II) with biosensitive macrocyclic ligands. Mycobiology 34(4):214–218

Rao PNP, Knaus EE (2008) COX-Evolution of nonsteroidal anti-inflammatory drugs (NSAIDs): cyclooxygenase (COX) inhibition and beyond. J Pharm Pharm Sci 11(2):81s–110s

Roubaty JL, Revillon A, Breant M (1977) A polarographic study of the pyridine-copper-chloride complexes in methanol and determination of the stability constants. Talanta 24(11):688–690

Roy TG, Hazari SK, Dey BK, Meah HA, Rahman MS, Kim DI et al. (2007) Synthesis, electrolytic behaviour and antimicrobial activities of cadmium complexes of isomers of 3,10-C- meso -3,5,7,7,10,12,14,14-octamethyl-1,4,8,11-tetraazacyclotetradecane. J Coord Chem 60(14):1567–1578

Roy TG, Hazari SK, Dey BK, Miah HA, Olbrich F, Rehder D (2007) Synthesis and antimicrobial activities of isomers of N(4),N(11)-Dimethyl-3,5,7,7,10,12,14,14-octamethyl-1,4,8,11-tetraazacyclotetradecane and their nickel(II) complexes. Inorg Chem 46 (13):5372–5380

Santra A, Mondal G, Acharjya M, Bera P, Panja A, Mandal TK, Mitra P, Bera P (2016) Catechol oxidase mimetic activity of copper(I) complexesof 3,5-dimethyl pyrazole derivatives: Coordination behavior, X-ray crystallography and electrochemical study. Polyhedron1 13:5–15

Sheldrick GM (2001) SHELXTL (Version 6.12) Structure Analysis Program. Bruker AXS Inc, Madison, Wisconsin

Singh K, Kumar Y, Puri P, Kumar M, Sharm C (2012) Cobalt, nickel, copper and zinc complexes with 1,3-diphenyl-1H-pyrazole-4-carboxaldehyde Schiff bases: antimicrobial, spectroscopic, thermal and fluorescence studies. Eur J Med Chem 52:313–321

Sobiesiak M, Muzioł T, Rozalski M, Krajewska U, Budzisz E (2014) Co(II), Ni(II) and Cu(II) complexes with phenylthiazole and thiosemicarbazone-derived ligands: synthesis, structure and cytotoxic effects. New J Chem 38:5349–5361

Tavares LS, Silva CSF, de Souza VC, da Silva VL, Diniz CG, Santos MO (2013) Strategies and molecular tools to fight antimicrobial resistance: resistome, transcriptome, and antimicrobial peptides. Front Microbiol 4:412–218

Tomalia DA (2009) In quest of a systematic framework for unifying and defining nanoscience. J Nanopart Res 11:1251–1310

Vanden Berghe DA, Vlietinck AJ (1991) Screening methods for antibacterial and antiviral agents from higher plants. In: Dey PMp, Harbone J B (eds) Methods in plant biochemistry. Academic, London, p 47–69

Viveka S, Dinesha, Shama P, Naveen S, Lokanath NK, Nagaraja GK (2015) Design, synthesis, anticonvulsant and analgesic studies of new pyrazole analogues: a Knoevenagel reaction approach. RSC Adv 5:94786–94795

Wade D, Silveira A, Rollins-Smith L, Bergman T, Silberring J, Lankinen H (2001) Hematological and antifungal properties of temporin A and a cecropin A-temporinA hybrid. Acta Biochim Pol 48:1185–1189